International Immunopharmacology 72 (2019) 496–503

Contents lists available at ScienceDirect

International Immunopharmacology

journal homepage: www.elsevier.com/locate/intimp

LncRNA H19/miR-let-7 axis participates in the regulation of ox-LDL-induced endothelial cell injury *via* targeting periostin

Lei Cao[a], Zhe Zhang[b], Yong Li[c], Peiyong Zhao[a], Yuguo Chen[c,*]

[a] Department of Cardiovascular, Weihai Municipal Hospital, Weihai 264200, Shandong Province, China
[b] Department of General medical, Weihai Municipal Hospital, Weihai 264200, Shandong Province, China
[c] Department of Emergency, Qilu Hospital of Shandong University, Jinan 250014, Shandong Province, China

ARTICLE INFO

Keywords:
Ox-LDL
Endothelial cell dysfunction
lncRNA H19
microRNA let-7
Periostin

ABSTRACT

Oxidized-low density lipoprotein (ox-LDL)-induced endothelial cell dysfunction is a crucial event in the pathogenesis of atherosclerosis (AS). Long noncoding RNAs (lncRNAs) have been shown to play important roles in this process. The purpose of this study was to investigate the biological effects of lncRNA H19 on the ox-LDL-induced endothelial cell injury and to explore the underlying molecular mechanisms. In the present study, the expression of H19 in the serum of patients with AS and in the ox-LDL-treated human umbilical vein endothelial cells (HUVECs) was significantly up-regulated. H19 knockdown by transfection with H19 siRNAs in ox-LDL-treated HUVECs remarkably promoted cell viability, suppressed the secretion of interleukin (IL)-1β, IL-6, and tumour necrosis factor (TNF)-α, decreased the expression of vascular cell adhesion molecule 1 (VCAM1), intercellular adhesion molecule 1 (ICAM1) and E-selectin, reduced levels of reactive oxygen species (ROS) and malondialdehyde (MDA), increased superoxide dismutase (SOD) levels, and reduced cell apoptosis. Moreover, H19 knockdown significantly down-regulated the ox-LDL-induced expression of periostin, but did not affect the expression of let-7a, which directly targets the 3′-UTR of periostin mRNA. In addition, periostin overexpression partly reversed the biological effects of H19 knockdown in ox-LDL-treated HUVECs, which were almost recapitulated by let-7 overexpression. In conclusion, these data suggest that H19 knockdown suppressed ox-LDL-induced inflammation, apoptosis and oxidative stress in HUVECs, which may be related to the down-regulation of periostin by interfering with let-7 bioavailability.

1. Introduction

Atherosclerosis (AS) is a multistep cardiovascular disease that is promoted by several risk factors, such as hypertension, hyperglycaemia, hyperlipidaemia, smoking and drinking [1]. Endothelial cell injury has been reported to be a key early event in the pathogenesis of AS, which is a complex process that includes apoptosis, inflammation, and oxidative stress [2,3]. Previous studies have shown that oxidized low-density lipoprotein (ox-LDL) is an important factor in the occurrence and development of AS, and there is an obvious increase in ox-LDL in the lesions of AS [4]. In the early stage of AS, ox-LDL promotes the formation of foam cells, and releases a large number of inflammatory factors, which further aggravates the course of AS [5,6]. Therefore, studies targeting ox-LDL-induced endothelial cell injury can further elucidate the pathogenesis of AS.

LncRNAs are transcripts longer than 200 nucleotides, which play important roles in various biological and pathological processes by interacting with multiple molecules, including DNA, RNA, and proteins [7]. H19, as an lncRNA, has been shown to act either as a tumour suppressor or oncogene, being involved in the development of multiple cancers [8,9]. In recent years, it has been found that H19 can also participate in the regulation of cardiovascular diseases, such as diabetic cardiomyopathy [10] and even AS [11]. However, the mechanisms of action of H19 in AS need more detailed explanations. MiRNAs are a class of 18–22 nucleotides long, non-coding RNAs, which have been identified as negative regulators of gene expression at the post-transcriptional level [12]. It has been reported that H19 harbours both canonical and non-canonical binding sites for the let-7 family of microRNAs, which plays important roles in regulating inflammation in diabetes-associated AS [13]. H19 acts as a molecular sponge to modulate let-7 availability [14]. Therefore, we speculated that H19 may modulate ox-LDL-induced endothelial cell injury by interacting with

* Corresponding author at: Department of Emergency, Qilu Hospital of Shandong University, No.107 West Culture Road, Lixia District, Jinan 250014, Shandong Province, China.
E-mail address: YuguoChencyg@163.com (Y. Chen).

https://doi.org/10.1016/j.intimp.2019.04.042
Received 30 September 2018; Received in revised form 19 April 2019; Accepted 19 April 2019
Available online 01 May 2019

let-7.

MiRNAs are incorporated into the RNA-induced silencing complex and bind to the seed sequence in the 3′-untranslated regions (3′-UTRs) of their target mRNAs to silence gene translation *via* mRNA degradation and/or translational repression. Periostin was shown to be a target gene of let-7. Periostin is a 90-kDa secreted matricellular protein that can alter extracellular matrix (ECM) remodelling in response to tissue injury. The dysregulation of periostin has been involved in a variety of disorders, including cancers [15,16], inflammatory diseases [17,18] and cardiovascular diseases [19,20]. One study has proved that periostin acts as a regulator of AS lesion formation and progression, suggesting that periostin could be a therapeutic target for AS plaque formation through modulation of the immune response and ECM remodelling [21]. Thus, we speculated that the H19/let-7/periostin axis may play a crucial role in ox-LDL-induced endothelial cell injury.

In the present study, we aimed to investigate the effects of H19 in ox-LDL-treated endothelial cells by assessing cell viability, apoptosis, inflammatory factor secretion and oxidative stress, and to further investigate whether the action of H19 was associated with the let-7/periostin axis.

2. Materials and methods

2.1. Patients

Twenty serum samples from patients with AS and 20 serum samples from healthy volunteers were collected at Weihai Municipal Hospital. Informed consent was obtained from all patients and healthy volunteers. The study was approved by the ethics committee of Weihai Municipal Hospital.

2.2. Cell culture and treatment

Human umbilical vein endothelial cells (HUVECs, Cat. No.: CRL-1730) were purchased from American Type Culture Collection (ATCC, Manassas, Virginia, USA), and they were used in the main text. Primary human umbilical vein endothelial cells (HUVECs, Cat. No.: PCS-100-010) and HUVEC/TERT 2 (Cat. No.: CRL-4053) were purchased from ATCC, and they were used in supplementary materials. HUVECs are cells derived from the endothelium of veins from the umbilical cord. They are used as a laboratory model system for study of the function and pathology of endothelial cells [22]. They were cultured in DMEM (Invitrogen, Carlsbad, CA, USA) supplemented with 10% foetal bovine serum (Sigma-Aldrich, St. Louis, MO, USA), 100 U/ml penicillin and 100 μg/ml streptomycin. Cells were cultured in a humidified atmosphere containing 5% CO_2 at 37 °C. HUVECs were treated with 100 μg/ml ox-LDL for 12 h, 18 h and 24 h for the subsequent experiments.

2.3. Cell transfection

H19 siRNAs and siRNA negative control (si-NC), let-7a mimics and mimic negative control (mimic-NC) were purchased from GenePharma (Shanghai, China). PcDNA3.1-periostin plasmids were constructed by Sangon Biotech (Shanghai, China). The transfection was performed using Lipofectamine 2000 (Invitrogen) when the cells reached 70% confluence according to the manufacturer's instructions.

2.4. Quantitative real-time PCR (qRT-PCR)

Total RNA was isolated from serum samples and cells using Trizol reagent according to the manufacturer's guidelines. RNA was reverse transcribed into cDNA using a Prime-Script RT-PCR kit (TaKaRa, Dalian, China). The expression of H19 and periostin was analysed by using SYBR Premix Ex Taq kit (Takara), and GAPDH was used as an endogenous control. The expression of let-7 was analysed by using TaqMan microRNA assays (Applied Biosystems, Foster City, CA, USA), and U6 was used as an endogenous control. qRT-PCR was performed on an HT7900 Real-Time PCR System (Applied Biosystems). The relative expression was calculated using the $2^{-\Delta\Delta Ct}$ method.

2.5. Cell viability assay

The cell viability was detected by MTT assay. Briefly, the HUVECs were cultured in 96-well plates. After cell transfection followed by ox-LDL treatment for 24 h, 10 μl of MTT solution (Millipore, Billerica, MA, USA) was added to each well, followed by incubation for 4 h. Then 150 μl of DMSO was added to dissolve for 15 min. Optical density was measured at 490 nm using a microplate reader.

2.6. Enzyme-linked immunosorbent assay (ELISA)

Levels of interleukin (IL)-1β, IL-6, tumour necrosis factor (TNF)-α of cell culture supernatants were determined by ELISA (Beyotime Biotechnology, Shanghai, China) following the manufacturer's instructions.

2.7. Western blot analysis

Total protein was extracted from cells using RIPA buffer containing protease and phosphatase inhibitors. Protein concentration was quantified using the BCA protein assay kit (Pierce, Rockford, IL, USA). Then, the protein samples were separated by SDS-PAGE and transferred onto polyvinylidene difluoride (PVDF) membranes (Millipore). After blocking with 5% non-fat milk at room temperature, the membranes were incubated with primary antibodies at 4 °C overnight: anti-VCAM1 (Abcam, Cambridge, MA, USA), anti-ICAM1 (Abcam), anti-E-selectin (Sigma-Aldrich, Saint Louis, MI, USA), anti-p-p65 (Cell Signaling Technology, Danvers, MA, USA), anti-p-IκB-α (Cell Signaling Technology), anti-Nrf2 (Cell Signaling Technology), anti-HO-1 (Cell Signaling Technology), anti-cleaved Caspase-3 (Cell Signaling Technology), anti-periostin (Abcam) and anti-GAPDH (ZSGB-BIO, Beijing, China), followed by incubation with horseradish peroxidase-conjugated secondary antibodies (ZSGB-BIO) at room temperature for 1 h. Signals were detected using ECL reagent (Millipore), and the relative intensities of protein blots were quantified using Image J software.

2.8. ROS measurement

Reactive oxygen species (ROS) levels were determined by 2,7-dichlorodihydrofluorescein diacetate probes (DCHF-DA, Beyotime Biotechnology). DCHF-DA can be oxidized to the fluorescent 2,7-dichlorofluorescein (DCF). Briefly, cells were incubated with 10 μM DCHF-DA for 20 min and then analysed by flow cytometry.

2.9. Measurement of SOD and MDA levels

The production of malondialdehyde (MDA) and superoxide dismutase (SOD) was determined by commercial kits (Jiancheng Biotech, Nanjing, China) according to the manufacturer's guidelines.

2.10. Apoptosis analysis

Cellular apoptosis was determined using the Annexin V-FITC/PI apoptosis detection kit (Jiancheng Biotech). HUVECs were seeded in 6-well plates. After cell transfection followed by ox-LDL treatment for 24 h, the cells were washed in PBS and resuspended in binding buffer. Then the cells were labelled with Annexin V-FITC and PI at room temperature in the dark for 20 min. The apoptosis rates were analysed using a FACSCalibur (Becton Dickinson, San Jose, CA, USA) within 1 h.

2.11. Dual-luciferase reporter assay

The 3′-UTR fragment of periostin containing the let-7a binding site was amplified by PCR using human cDNA as a template, and then cloned into a psiCHECK2 vector opened with *Xho*I and *Not*I, and named psiCHECK2-periostin. Mutations in the 3′-UTR of periostin with let-7a target site were generated with the QuickChange Site-Directed Mutagenesis kit (Stratagene, La Jolla, CA, USA), and named psiCHECK2-periostin mut. HUVECs were seeded into 48-well plates, and co-transfected the indicated luciferase reporter and let-7a mimic or mimic-NC using Lipofectamine 2000. Forty-eight hours after transfection, the luciferase activities were measured using the Dual-Luciferase Reporter Assay (Promega, Madison, WI, USA) according to the manufacturer's protocol. Renilla luciferase (Rluc) activity was normalised against Firefly luciferase activity.

2.12. Statistical analysis

All experiments were performed at least in triplicate. The statistical analysis was performed using GraphPad Prism software. Data are presented as the mean ± standard deviation (SD). Comparisons between 2 groups were analysed by the *t*-test, and comparisons between > 2 groups were analysed by one-way analysis of variance followed by the Bonferroni test. $p < 0.05$ was considered to be statistically significant.

3. Results

3.1. H19 was up-regulated in AS patients and ox-LDL-induced HUVECs

We first examined the expression of H19 in the serum of AS patients and normal controls. As shown in Fig. 1A, the H19 expression in AS patients was significantly ($p < 0.05$) up-regulated compared with that in the normal controls. We further treated HUVECs with ox-LDL to induce endothelial cell injury, as shown in Fig. 1B; the H19 expression was gradually increased in a time-dependent manner. To investigate the effects of H19 in the ox-LDL-treated HUVECs, we used H19 siRNAs to knockdown its expression (Fig. 1C). The cell viability analysis showed that, compared with the untreated group, ox-LDL treatment induced a significant reduction ($p < 0.05$); H19 knockdown markedly ($p < 0.05$) elevated the cell viability compared with the ox-LDL group (Fig. 1D).

3.2. H19 knockdown suppressed ox-LDL-induced inflammation

To investigate the effects of H19 in the ox-LDL-treated HUVECs, we first measured the expression levels of inflammatory cytokines by ELISA and Western blot. As shown in Fig. 2A–C, compared with the untreated group, ox-LDL treatment induced increased levels of IL-1β, IL-6, TNF-α, which were significantly ($p < 0.05$) suppressed by the knockdown of H19. Similar results were obtained in two alternative HUVEC cell lines (Supplementary Fig. 1 and Fig. 2). We further measured the protein levels of adhesion molecules, the data are shown in Fig. 2D–G. H19 knockdown markedly ($p < 0.05$) suppressed the ox-LDL-induced increased expression of VCAM1, ICAM1 and E-selectin. Moreover, we detected the protein levels related with classical NF-κB inflammatory signaling. As shown in Fig. 2H and I, compared with untreated group, the levels of p-p65 and p-IκB-α were obviously ($p < 0.05$) elevated in the ox-LDL group. Compared with the ox-LDL group, the levels of p-p65 and p-IκB-α were significantly ($p < 0.05$) decreased in the si-H19 + ox-LDL group.

3.3. H19 knockdown suppressed ox-LDL-induced oxidative stress and cell apoptosis

We further assessed the effects of H19 on the oxidative stress by detecting the production levels of ROS, SOD and MDA. As shown in Fig. 3A–C, ox-LDL treatment induced oxidative stress, including elevated ROS and MDA levels, and decreased SOD level. Compared with the ox-LDL group, H19 knockdown remarkably ($p < 0.05$) decreased ROS and MDA levels, and inhibited the decline of SOD production

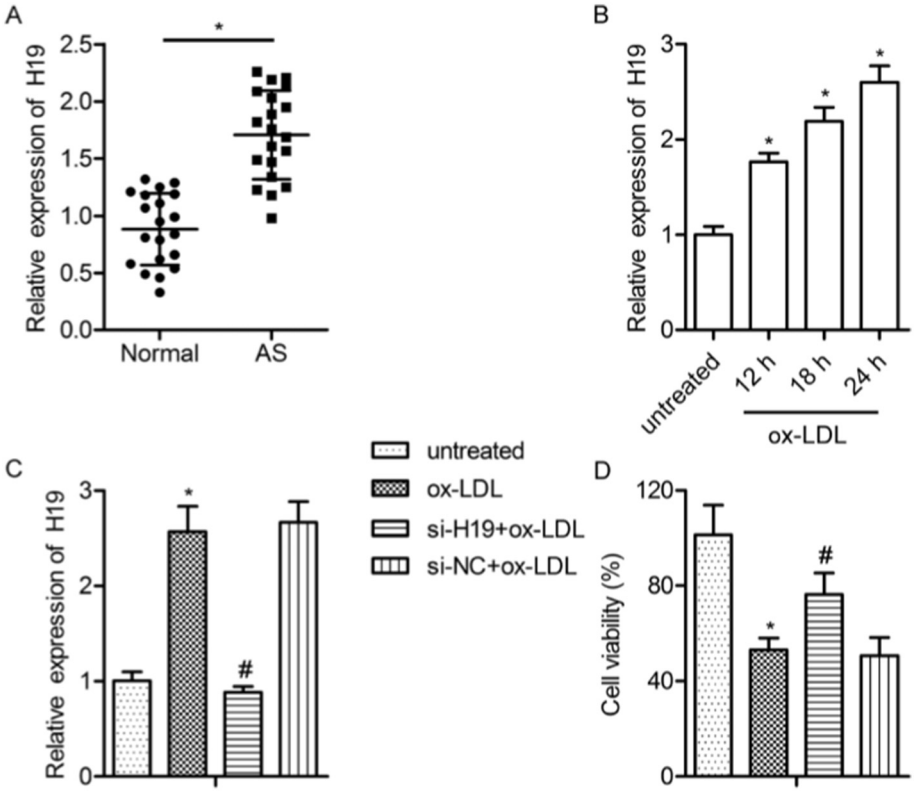

Fig. 1. H19 was up-regulated in AS patients and ox-LDL-induced HUVECs. (A) The expression levels of H19 in the serum of 20 pairs of AS patients and normal controls were detected using RT-PCR and normalised to GAPDH levels. (B) The HUVECs were treated with 100 μg/ml ox-LDL for 12, 18 and 24 h. The expression levels of H19 were detected using RT-PCR. (C) Untreated group, normal cultured HUVECs; ox-LDL group, HUVECs treated with ox-LDL for 24 h; si-H19 + ox-LDL group, HUVECs transfected with H19 siRNAs for 24 h, followed by treatment with ox-LDL for 24 h; si-NC + ox-LDL group, HUVECs transfected with H19 siRNA negative control for 24 h, followed by treatment with ox-LDL for 24 h. The expression levels of H19 were detected using RT-PCR. (D) The cell viability was examined by MTT assay. $n = 4$, $^*p < 0.05$ *vs.* normal or untreated group, $\#p < 0.05$ *vs.* ox-LDL group.

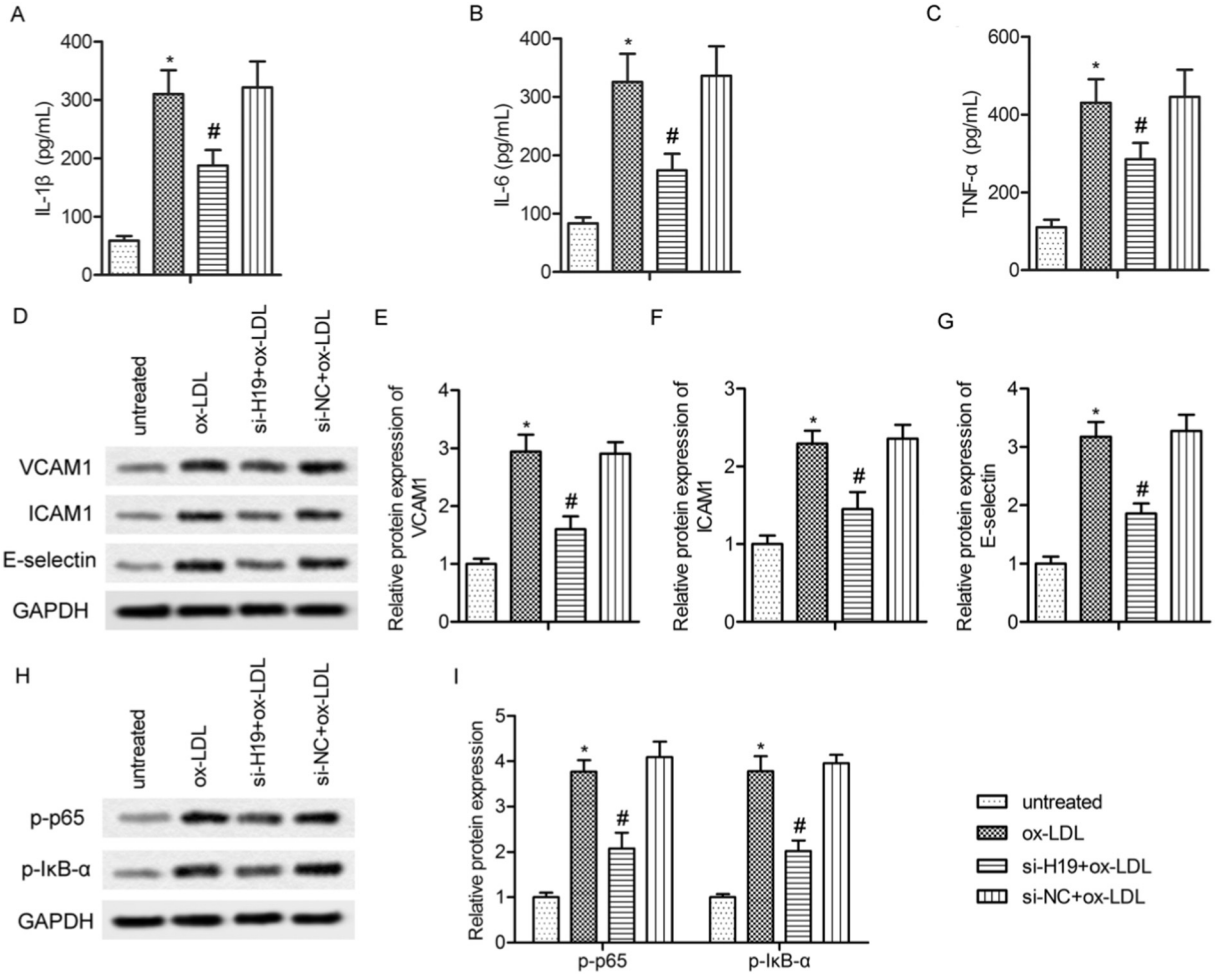

Fig. 2. H19 knockdown suppressed ox-LDL-induced inflammation. The secreted levels of IL-1β (A), IL-6 (B) and TNF-α (C) were detected by ELISA. (D) The protein expression levels of VCAM1, ICAM1 and E-selectin were detected by Western blot assay and normalised to GAPDH expression. The relative protein expression of VCAM1 (E), ICAM1 (F) and E-selectin (G) are indicated by histograms. (H) The protein levels of p-p65 and p-IκB-α were detected by Western blot assay and the relative protein expression are indicated by histograms (I). $n = 3$, $^{*}p < 0.05$ *vs.* untreated group, $\#p < 0.05$ *vs.* ox-LDL group.

caused by ox-LDL treatment. Similar results were obtained in two alternative HUVEC cell lines (Supplementary Fig. 1 and Fig. 2). The flow cytometry analysis showed that, compared with the untreated group, ox-LDL treatment significantly ($p < 0.05$) elevated the cell apoptosis, which was suppressed by H19 knockdown (Fig. 3D and E). Furthermore, we measured the protein levels related with antioxidant Nrf2/HO-1 signaling and cell apoptosis. As shown in Fig. 3F–H, compared with the untreated group, the expression of Nrf2 and HO-1 was significantly ($p < 0.05$) down-regulated, while the level of cleaved Caspase-3 was remarkably ($p < 0.05$) up-regulated in the ox-LDL group. H19 knockdown blocked the reduction of Nrf2 and HO-1 induced by ox-LDL treatment, but down-regulated the increased level of cleaved Caspase-3 caused by ox-LDL treatment.

3.4. H19 regulated periostin expression by antagonising let-7

As H19 has been reported to act as a "sponge" to sequester let-7 [14], and periostin was predicted to be a target gene of let-7, we measured the expression levels of let-7a and periostin in ox-LDL-treated HUVECs. As shown in Fig. 4A–C, ox-LDL treatment induced decreased levels of let-7a, and increased mRNA and protein expression of periostin. Compared with the ox-LDL group, the expression of periostin was significantly ($p < 0.05$) down-regulated in the si-H19 + ox-LDL group; however, the expression level of let-7a was not affected by H19 knockdown, suggesting that H19 may regulate periostin expression by antagonising let-7 bioavailability. Similar results were obtained in two alternative HUVEC cell lines (Supplementary Fig. 3 and Fig. 4). To confirm the target relationship between let-7 and periostin, a dual-luciferase reporter assay was performed. As shown in Fig. 4D, the Rluc activity decreased in response to let-7a overexpression in the HUVECs containing psiCHECK2-periostin; and the decreased Rluc activity of psiCHECK2-periostin mut in response to let-7a overexpression was not observed, confirming that let-7a directly targeted at the 3′-UTR of periostin to regulate its expression. Furthermore, the mRNA and protein expression of periostin was down-regulated by let-7a overexpression (Fig. 4E and F).

3.5. Let-7a/periostin axis was involved in the biological roles of H19 in ox-LDL-induced HUVECs

To further elucidate whether the biological roles of H19 were associated with the regulation of let-7/periostin axis, we transfected HUVECs with the combination of si-H19 and pcDNA3.1-periostin plasmids, or let-7a mimic, followed by the ox-LDL treatment. The secretion of inflammatory cytokines, the ROS level and the cell apoptosis was detected. As shown in Fig. 5, compared with si-H19 group, the up-regulated levels of IL-1β, IL-6 and TNF-α, the elevated ROS production and the increased cell apoptosis rate were detected in the si-H19 + periostin group, suggesting that periostin overexpression partly reversed the effects of H19 knockdown in the ox-LDL-induced HUVECs.

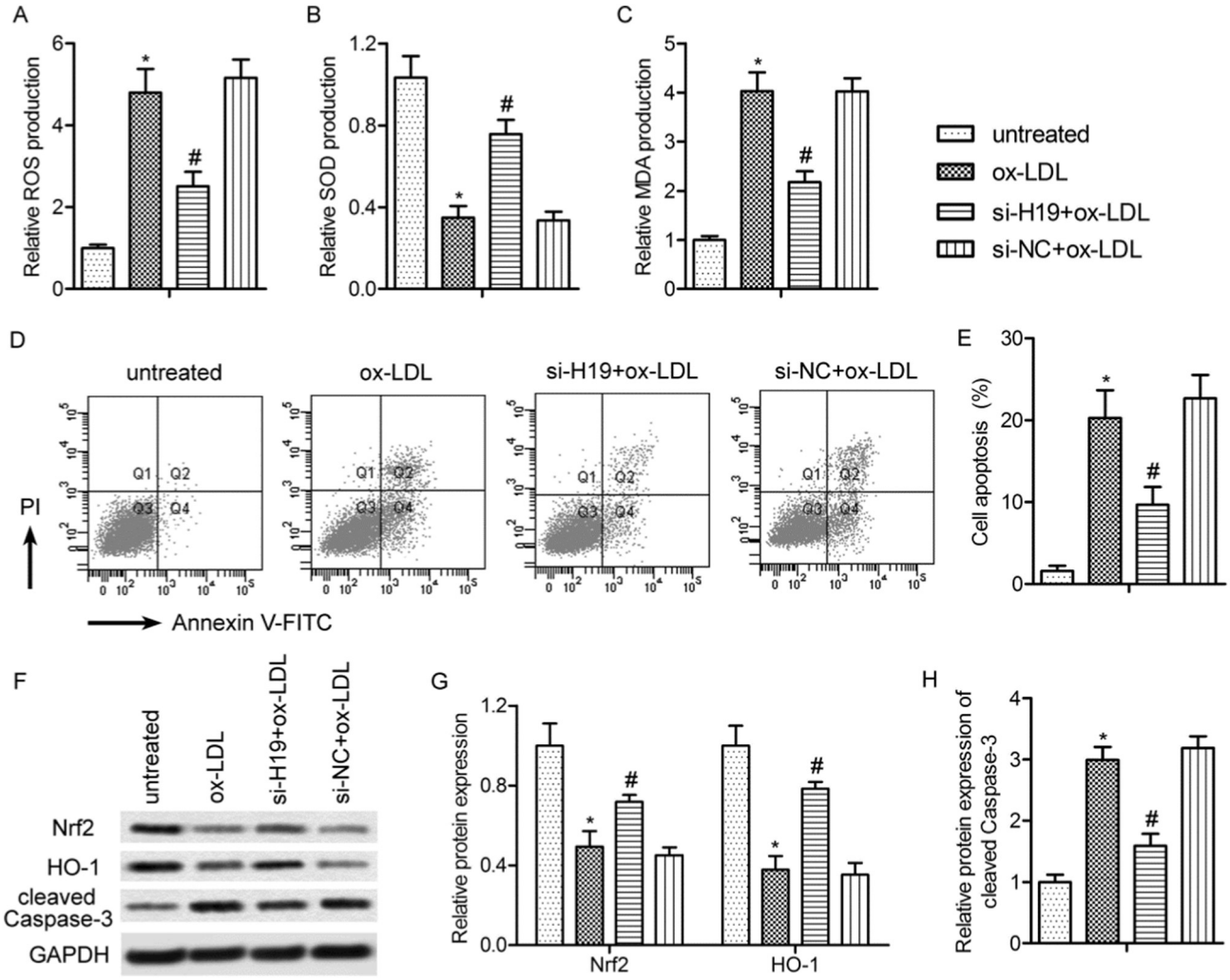

Fig. 3. H19 knockdown suppressed ox-LDL-induced oxidative stress and cell apoptosis. (A) ROS production was measured by flow cytometry using DCHF-DA probes. SOD (B) and MDA (C) levels were detected by commercial kits and are indicated by histograms. Cell apoptosis was measured by flow cytometry (D) and indicated by histograms (E). (F) The protein expression levels of Nrf2, HO-1 and cleaved Caspase-3 were detected by Western blot assay. The relative protein expression of Nrf2 and HO-1 (G), and cleaved Caspase-3 (H) are indicated by histograms. $n = 3$, $^{*}p < 0.05$ *vs.* untreated group, $\#p < 0.05$ *vs.* ox-LDL group.

Moreover, the biological effects caused by H19 knockdown were almost recapitulated by let-7 overexpression, including the down-regulated levels of IL-1β, IL-6 and TNF-α, the decreased ROS production and the reduced cell apoptosis. These results suggest that H19 regulates ox-LDL-induced inflammation, apoptosis and oxidative stress, at least partly *via* modulating the let-7a/periostin axis.

4. Discussion

At present, AS is still one of the leading causes of mortality in the world, despite great advances in both basic and clinical research [23,24]. In recent years, the roles of non-coding RNA in endothelial function and AS have attracted increasing attention. Chen et al. have reported that lncRNA GAS5 was significantly increased in the plaque of atherosclerosis, which regulates the apoptosis of macrophages and endothelial cells *via* exosomes [25]. Yong et al. revealed that lncRNA MALAT1 protects the endothelium from ox-LDL-induced endothelial cell dysfunction partly through competing with miR-22-3p for endogenous RNA, thus up-regulating the expression of the miR-22-3p target genes CXCR2 and AKT [26]. Pan has shown that H19 promotes AS by regulating the MAPK and NF-kB signaling pathway [11]. In the present study, we further investigated the biological roles of H19 in the ox-LDL-induced endothelial cell injury and clarified its underlying mechanism.

Consistent with Pan's study [11], we found that H19 was highly expressed in the serum of patients with AS, confirming its crucial role in AS. We further showed that H19 expression was significantly increased in ox-LDL-treated HUVECs, which characterised by endothelial cell injury, including increased inflammatory factors, cell apoptosis and oxidative stress [6,27]. Inflammation plays an important role during the progression of endothelial dysfunction. The expression of inflammatory cytokines, including inflammatory factors and cell adhesion molecules, can promote the adhesion of monocytes to the vascular endothelium, leading to the activation of macrophages; these macrophages then absorb lipoprotein, resulting in foam cell formation, which further stimulates vascular inflammation [28,29]. In the present study, we found that the elevated levels of IL-1β, IL-6, TNF-α, VCAM1, ICAM1 and E-selectin induced by ox-LDL were all suppressed by the knockdown of H19. NF-κB is the critical transcription factor that mediates the inflammatory response, and it is activated through I-κBα phosphorylation, and then translocates to the nucleus. We further found that ox-LDL induced the increased levels of p-IκB-α and p-p65, implying the activation of NF-κB signaling. Compared with the ox-LDL group, the levels of p-p65 and p-IκB-α were significantly decreased by the knockdown of H19, implying the suppression of NF-κB activation. These results demonstrate that H19 knockdown protects the endothelial

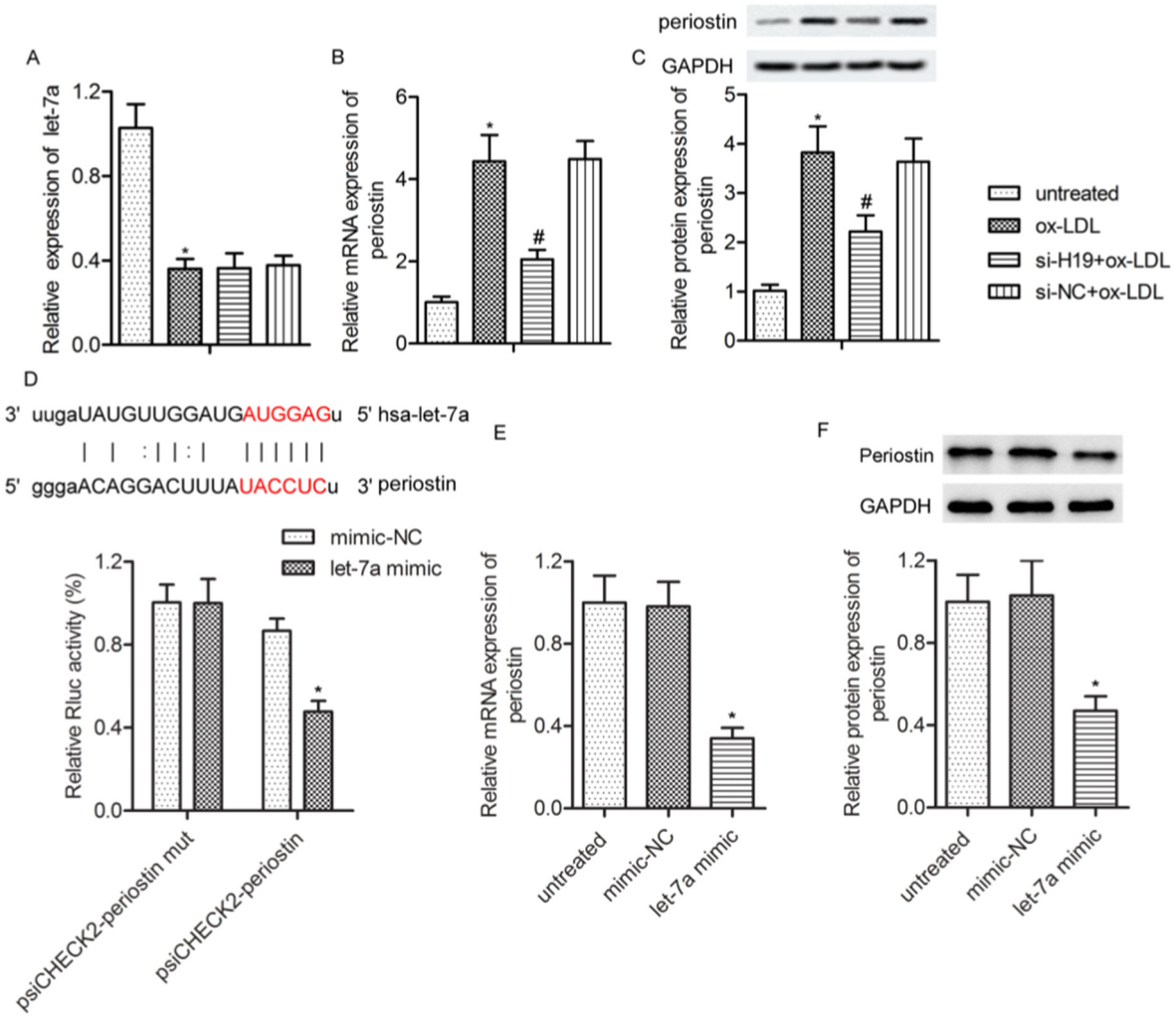

Fig. 4. H19 acts as a molecular sponge for let-7 to regulate periostin expression. (A) The expression level of let-7a was detected by RT-PCR assay and normalised to U6 levels. The mRNA (B) and protein (C) expression of periostin were detected by RT-PCR and Western blot assay, respectively. *$p < 0.05$ *vs*. untreated group, #$p < 0.05$ *vs*. ox-LDL group. (D) Predicted 3′-UTR sequence of periostin containing the let-7a binding sites. The psiCHECK2-periostin or psiCHECK2-periostin mut plasmids were co-transfected into HUVECs with the let-7a mimic or mimic-NC. The Rluc activity was analysed by dual-luciferase reporter assay 48 h post-transfection. The mRNA (E) and protein (F) expression of periostin in HUVECs transfected with let-7a mimic or mimic-NC were detected by RT-PCR and Western blot assay, respectively. $n = 4$, *$p < 0.05$ *vs*. mimic-NC group.

cells against ox-LDL-induced inflammation.

Oxidative stress, known as the increased bioactivity of ROS relative to antioxidant defences, has been shown to be an important event in endothelial cell dysfunction [30]. Nrf2 is an important transcription factor regulating several antioxidant enzyme genes, such as HO-1 [31]. HO-1 is regarded as an antioxidative and cytoprotective enzyme [32,33]. In the present study, the knockdown of H19 was found to suppress ox-LDL-induced oxidative stress by decreasing ROS and MDA levels, and inhibited the decline of SOD production. Meanwhile, the reduction of Nrf2 and HO-1 caused by ox-LDL treatment was also blocked by H19 knockdown. It has been reported that oxidative stress is closely associated with various pathological processes, including inflammation and apoptosis. Endothelial cell apoptosis can destroy the structure and function of the endothelium, accelerating the formation of foam cells [34]. During mitochondrial apoptosis, active cleaved Caspase-3 increases, which contributes to the cleavage of cellular target proteins [35]. As we have shown, the ox-LDL-induced cell apoptosis and increased cleaved caspase-3 were suppressed by H19 knockdown. These results demonstrate that H19 knockdown protects endothelial cells against ox-LDL-induced oxidative stress and apoptosis.

LncRNAs can act as “sponges” to bind specific miRNAs and regulate their function [36,37] by modulating the expression of their target genes [38]. Kallen et al. reported that the conserved, imprinted lncRNA H19 could bind to let-7 and interferes with its function, acting as a natural molecular sponge for let-7 [14]. The H19/let-7 axis has been shown to play important roles in many biological processes, such as tumorigenesis [39], the production of steroids [40] and glucose metabolism [41]. Subsequent bioinformatic analysis and dual-luciferase reporter assay confirmed that let-7 directly targets the 3′-UTR of periostin mRNA. Actually, low levels of periostin are detected in various adult tissues at baseline, but dramatically increased expression and secretion are found with acute injury [42,43]. In the present study, H19 knockdown significantly down-regulated the ox-LDL-induced periostin expression, but did not affect the expression level of let-7a, suggesting that H19 knockdown inhibited the expression of periostin at least partly *via* modulating the bioavailability of let-7, but not its expression; this was consistent with the previous result H19 regulates gene expression by antagonising let-7. Thus, we speculated that regulation of the let-7a/periostin axis was involved in the biological roles of H19. The detection of inflammatory factor secretion, ROS levels and cell apoptosis showed that periostin overexpression partly reversed the biological effects of H19 knockdown, which were almost recapitulated by let-7a overexpression (elevated let-7a bioavailability). Taken together, the above results suggest that H19 regulates the ox-LDL-induced inflammation,

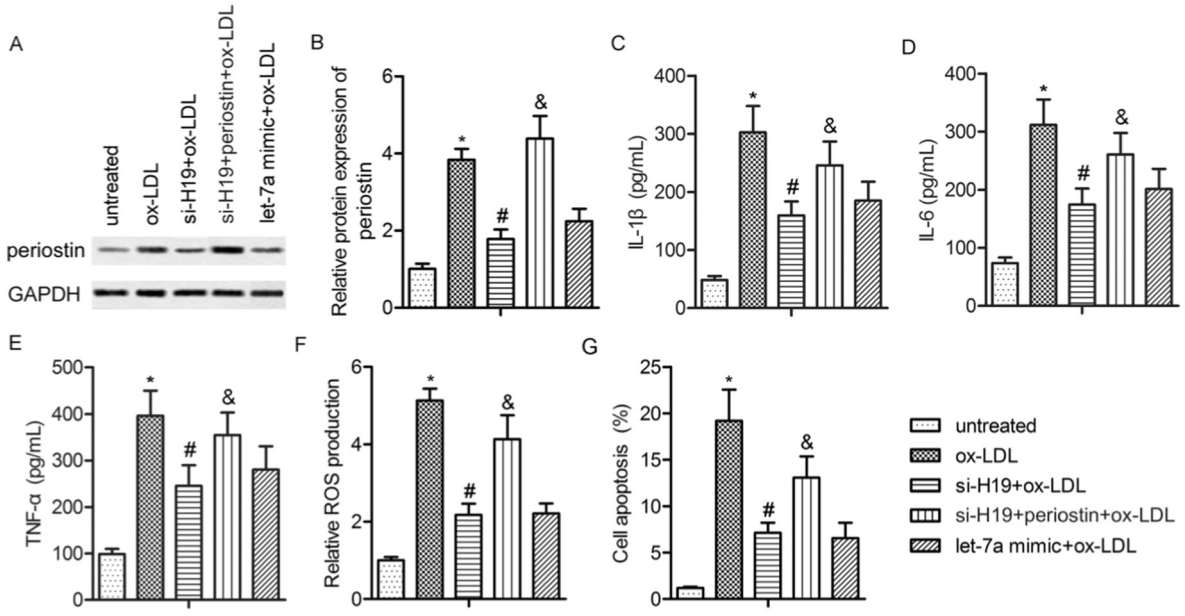

Fig. 5. Let-7/periostin axis was involved in the biological roles of H19 in ox-LDL-induced HUVECs. HUVECs were transfected with si-H19 alone, or the combination of si-H19 and pcDNA3.1-periostin plasmids, let-7a mimic for 24 h, followed by the ox-LDL treatment. (A) The protein expression levels of periostin were detected by Western blot assay. (B) The relative protein expression of periostin is indicated by histograms. The secreted levels of IL-1β (C), IL-6 (D) and TNF-α (E) were assessed by ELISA. (F) ROS production was measured by flow cytometry using DCHF-DA probes. (G) Cell apoptosis was measured by flow cytometry. $n = 4$, $*p < 0.05$ *vs.* untreated group, $\#p < 0.05$ *vs.* ox-LDL group, $\&p < 0.05$ *vs.* si-H19 + ox-LDL group.

apoptosis and oxidative stress at least partly *via* interfering with let-7 bioavailability, and thus modulating periostin expression.

In summary, these results demonstrate that H19 was up-regulated in the serum of patients with AS. H19 knockdown suppressed ox-LDL-induced inflammation, apoptosis and oxidative stress in HUVECs, which may be related to the down-regulation of periostin by interfering with let-7 action. Therefore, targeting H19/let-7/periostin axis may reveal a potential therapeutic strategy for endothelial cell dysfunction.

Conflict of interest

The authors declare that they have no conflict of interest.

Appendix A. Supplementary data

Supplementary data to this article can be found online at https://doi.org/10.1016/j.intimp.2019.04.042.

References

[1] A.J. Lusis, Atherosclerosis, Nature 407 (2000) 233–241.
[2] J.M. Isner, M. Kearney, S. Bortman, J. Passeri, Apoptosis in human atherosclerosis and restenosis, Circulation 93 (1996) 394–395.
[3] E.A. Kaperonis, C.D. Liapis, J.D. Kakisis, et al., Inflammation and atherosclerosis, Circulation 16 (2002) 107–113.
[4] I. Tabas, K.J. Williams, J. Borén, Subendothelial lipoprotein retention as the initiating process in atherosclerosis update and therapeutic implications, Circulation 116 (2007) 1832–1844.
[5] H. Itabe, Oxidized low-density lipoprotein as a biomarker of in vivo oxidative stress: from atherosclerosis to periodontitis, J. Clin. Biochem. Nutr. 51 (2012) 1–8.
[6] N. Kume, T. Kita, Apoptosis of vascular cells by oxidized LDL: involvement of caspases and LOX-1 and its implication in atherosclerotic plaque rupture, Circ. Res. 94 (2004) 269–270.
[7] S. Arslan, Ö. Berkan, T. Lalem, et al., Long non-coding RNAs in the atherosclerotic plaque, Atherosclerosis 266 (2017) 176.
[8] T. Wu, L. Qu, G. He, et al., Regulation of laryngeal squamous cell cancer progression by the lncRNA H19/miR-148a-3p/DNMT1 axis, Oncotarget 7 (2016) 11553–11566.
[9] T. Yoshimizu, A. Miroglio, M.A. Ripoche, et al., The H19 locus acts in vivo as a tumor suppressor, Proc. Natl. Acad. Sci. U. S. A. 105 (2008) 12417–12422.
[10] X. Li, H. Wang, B. Yao, et al., lncRNA H19/miR-675 axis regulates cardiomyocyte apoptosis by targeting VDAC1 in diabetic cardiomyopathy, Sci. Rep. 6 (2016) 36340.
[11] J.X. Pan, LncRNA H19 promotes atherosclerosis by regulating MAPK and NF-kB signaling pathway, Eur. Rev. Med. Pharmacol. Sci. 21 (2017) 322–328.
[12] D.P. Bartel, MicroRNA target recognition and regulatory functions, Cell 136 (2009) 215.
[13] E. Brennan, B. Wang, A. Mcclelland, et al., Protective effect of let-7 miRNA family in regulating inflammation in diabetes-associated atherosclerosis, Diabetes 66 (2017) 2266–2277.
[14] N. Kallen Amanda, X.B. Zhou, J. Xu, et al., The imprinted H19 LncRNA antagonizes Let-7 MicroRNAs, Mol. Cell 52 (2013) 101–112.
[15] P.V. Nuzzo, A. Rubagotti, L. Zinoli, et al., The prognostic value of stromal and epithelial periostin expression in human breast cancer: correlation with clinical pathological features and mortality outcome, BMC Cancer 16 (2016) 95.
[16] L. Yang, L. Fan, G. Feng, et al., Periostin promotes tumor angiogenesis in pancreatic cancer via Erk/VEGF signaling, Oncotarget 7 (2016) 40148–40159.
[17] S.J. Koh, Y. Choi, B.G. Kim, et al., Matricellular protein periostin mediates intestinal inflammation through the activation of nuclear factor κB signaling, PLoS One 11 (2016) e0149652.
[18] Y. Huang, W. Liu, H. Xiao, et al., Matricellular protein periostin contributes to hepatic inflammation and fibrosis, Am. J. Pathol. 185 (2015) 786.
[19] J. Litvin, S. Zhu, R. Norris, R. Markwald, Periostin family of proteins: therapeutic targets for heart disease, Anat Rec A Discov Mol Cell Evol Biol 287A (2005) 1205–1212.
[20] N.M. Landry, S. Cohen, D. Imc, Periostin in cardiovascular disease and development: a tale of two distinct roles, Basic Res. Cardiol. 113 (1) (2018).
[21] J.A. Schwanekamp, A. Lorts, R.J. Vagnozzi, et al., Deletion of periostin protects against atherosclerosis in mice by altering inflammation and extracellular matrix remodeling Significance, Arterioscler. Thromb. Vasc. Biol. 36 (2016) 60–68.
[22] H.J. Park, Y. Zhang, S.P. Georgescu, et al., Human umbilical vein endothelial cells and human dermal microvascular endothelial cells offer new insights into the relationship between lipid metabolism and angiogenesis, Stem Cell Rev. 2 (2006) 93–101.
[23] D. Mozaffarian, E.J. Benjamin, A.S. Go, et al., Heart disease and stroke statistics—2015 update, Circulation 131 (2015) (CIR.0000000000000350).
[24] W.G. Members, D. Mozaffarian, E.J. Benjamin, et al., Heart disease and stroke statistics-2016 update: a report from the American heart association, Circulation e38 (2016) 133.
[25] L. Chen, W. Yang, Y. Guo, et al., Exosomal lncRNA GAS5 regulates the apoptosis of macrophages and vascular endothelial cells in atherosclerosis, PLoS One 12 (2017) e0185406.
[26] T. Yong, J. Xian, X. Yin, et al., The lncRNA MALAT1 protects the endothelium against ox-LDL-induced dysfunction via upregulating the expression of the miR-22-3p target genes CXCR2 and AKT, FEBS Lett. 589 (2015) 3189–3196.
[27] B. Hennig, C.K. Chow, Lipid peroxidation and endothelial cell injury: implications in atherosclerosis, Free Radic. Biol. Med. 4 (1988) 99.
[28] A.Y. Meliton, F. Meng, Y. Tian, et al., Oxidized phospholipids protect against lung injury and endothelial barrier dysfunction caused by heat-inactivated Staphylococcus aureus, Am. J. Physiol. Lung Cell. Mol. Physiol. 308 (2015) L550.
[29] K. Yamagata, A. Miyashita, H. Matsufuji, M. Chino, Dietary flavonoid apigenin inhibits high glucose and tumor necrosis factor alpha-induced adhesion molecule

expression in human endothelial cells, J. Nutr. Biochem. 21 (2010) 116–124.
[30] G. Zalba, A. Fortuño, J.G. San, et al., Oxidative stress, endothelial dysfunction and cerebrovascular disease, Cerebrovasc. Dis. 24 (2007) 24–29.
[31] X.L. Chen, G. Dodd, S. Thomas, et al., Activation of Nrf2/ARE pathway protects endothelial cells from oxidant injury and inhibits inflammatory gene expression, Am. J. Physiol. Heart Circ. Physiol. 290 (2006) H1862.
[32] A.O. Lawal, J.L. Marnewick, E.M. Ellis, Heme oxygenase-1 attenuates cadmium-induced mitochondrial-caspase 3- dependent apoptosis in human hepatoma cell line, BMC Pharmacol. Toxicol. 16 (2015) 1–13.
[33] C. Dong, H. Zheng, S. Huang, et al., Heme oxygenase-1 enhances autophagy in podocytes as a protective mechanism against high glucose-induced apoptosis, Exp. Cell Res. 337 (2015) 146–159.
[34] J.C. Choy, D.J. Granville, D.W. Hunt, B.M. Mcmanus, Endothelial cell apoptosis: biochemical characteristics and potential implications for atherosclerosis, J. Mol. Cell. Cardiol. 33 (2001) 1673–1690.
[35] S.J. Riedl, Y. Shi, Molecular mechanisms of caspase regulation during apoptosis, Nat. Rev. Mol. Cell Biol. 5 (2004) 897–907.
[36] M.S. Ebert, P.A. Sharp, Emerging roles for natural MicroRNA sponges, Curr. Biol. 20 (2010) R858–R861.
[37] L. Salmena, L. Poliseno, Y. Tay, et al., A ceRNA hypothesis: the Rosetta stone of a hidden RNA language? Cell 146 (2011) 353–358.
[38] M.R. Fabian, N. Sonenberg, The mechanics of miRNA-mediated gene silencing: a look under the hood of miRISC, Nat. Struct. Mol. Biol. 19 (2012) 586.
[39] C. Ma, K. Nong, H. Zhu, et al., H19 promotes pancreatic cancer metastasis by derepressing let-7's suppression on its target HMGA2-mediated EMT, Tumor Biol. 35 (2014) 9163–9169.
[40] Y. Men, Y. Fan, Y. Shen, et al., The steroidogenic acute regulatory protein (StAR) is regulated by the H19/let-7 Axis, Endocrinology 158 (2016) 402–409.
[41] Y. Gao, F. Wu, J. Zhou, et al., The H19/let-7 double-negative feedback loop contributes to glucose metabolism in muscle cells, Nucleic Acids Res. 42 (2014) 13799.
[42] P. Snider, R.B. Hinton, R.A. Morenorodriguez, et al., Periostin is required for maturation and extracellular matrix stabilization of noncardiomyocyte lineages of the heart, Circ. Res. 102 (2008) 752–760.
[43] D. Hakuno, N. Kimura, M. Yoshioka, et al., Periostin Advances Atherosclerotic and Rheumatic Cardiac Valve Degeneration by Inducing Angiogenesis and MMP Production in Humans and Rodents, Springer, Singapore, 2016.